Indonesian Journal on Health Science and Medicine
Vol. 2 No. 1 (2025): January
ISSN 3063-8186. Published by Universitas Muhamamdiyah Sidoarjo

https://doi.org/10.21070/ijhsm.v2i1.60

Spectroscopic, Anticancer and Theoretical Study of New Ligand Derived From (3-hydrazineylidenebutan-2-one oxime) and its Complex with Some Metal Ions

Israa Ali Abbas[1], Fayez Owaid Neamah[2]
[1] Department of Chemistry, College of Science, University of Thi-Qar, 64001 Nasiriya city, Iraq
[2] Directorate-General for Education Dhi Qar, Nassiriya 64001, Iraq
ORCID ID: https://orcid.org/0009-0008-6475-0448 , https://orcid.org/0009-0005-9812-7038

Email: is.al_ch@utq.edu.iq[1] , fayezawid@utq.edu.iq[2]

Abstract. The new Schiff base ligand derivate from 3-hydrazineylidenebutan-2-one oxime and its metal complexes were synthesized and characterized by analytical technique and spectroscopy method such as HNMR, FTIR and mass spectroscopy. The optimized geometric structures and HOMO-LUMO orbitals were computed by using DFT (density functional theory) at B3LYP/6-31G+(d,p) level. When the ligand's cytotoxic activity was tested against human breast cancer (MCF-7) and normal cells (WRL68), it was found to be more cytotoxic against MCF-7 but reasonably safe against normal cells.

Highlights:

1. ynthesis: Schiff base ligand and metal complexes characterized via spectroscopy techniques.
2. Computational: DFT calculated optimized structures, HOMO-LUMO orbitals at B3LYP/6-31G+ level.
3. Cytotoxicity: Ligand showed higher toxicity against MCF-7 cells, safe for normal cells.

Keywords: anticancer, complex, ligand, oxime, Schiff base.

Introduction

Schiff bases are compounds that include the azomethine group (-C=N-)[1]. Simply explained, they are the results of a chemical reaction between a ketone or aldehyde and an elementary amine under specific conditions[2]. Structurally, O of the carbonyl (C=O) group in a ketone or aldehyde is substituted with N in the amine group to form azomethine, or imine (C=N) functionality synthesis with the molecular release of H2O[3]. Even Hugo Schiff may not have realized, About 155 years ago, he published the findings of his research as scientific communication, predicting that these organic components would become a distinct area of intense interest in chemistry and other scientific disciplines that deal with materials, biological, physical and engineering[4]. Schiff bases

ISSN 3063-8186. Published by Universitas Muhamamdiyah Sidoarjo

https://doi.org/10.21070/ijhsm.v2i1.60

compounds have been shown to exhibit a broad range of biological activities including antibacterial[5], antifungal[6], anti-inflammatory[7], antipyretic[8], antimalarial[9], antiviral[10], antiproliferative[11], antitumor[12] and anticancer properties[13]. Schiff base is also employed as a mordent in dyeing processes [15] and as an inhibitor of corrosion [14]. Because schiff bases are stable in a variety of oxidative and reductive conditions, they are frequently employed as chelating ligands in main group and transition metal coordination chemistry. Imine ligands are on the borderline between hard and soft Lewis bases[16].

Oximes are identified by the atom of oxygen immediately linked to the atom of nitrogen with two free electrons. Oxime derivatives' biological action is linked to their N-OH groups, which is chelated to metal ions. The (−N−OH) moiety is adaptable to oxidation, reduction, and conjugation with inorganic and organic compounds. Oxime property of the α-adjacent atom with free electrons contributes to nucleophilic displacement processes via the anionic form N−O. Oxime ligands' ability to form a stable complex with various metal ions and create nitroxide radicals are significant, but not exclusive, the biological and toxicological action of oximes. For these properties, compounds containing oxime group have showed efficacy in a variety of medicinal applications, including antibacterial, antimalarial, and anticancer medications[17]. According to the unique properties of oxime, there is a growing interest in the synthesis and structural investigation of oxime derivatives in order to discover innovative therapeutic drugs[18]

Methods

All used materials have been obtained from Merck. Melting points were measured using Stuart SMP3. The magnetization susceptibility of the complexes has been examined at a room temperature via a Gouy balance. Shimadzu device was used to record FT-IR spectra in KBr disk ranging from 400-4000 cm-1. Micro-analyses (C.H.N) was used Vario ELV5 Elemental analyzer model 11086109 Germany. 1H-NMR was recorded on 400 MHz Bruker NMR spectrometer. Bibby conductometer type MCl was used for conductance measurements of complexes.

Indonesian Journal on Health Science and Medicine
Vol. 2 No. 1 (2025): January
ISSN 3063-8186. Published by Universitas Muhamamdiyah Sidoarjo

https://doi.org/10.21070/ijhsm.v2i1.60

Synthesis of 3-hydrazineylidenebutan-2-one oxime (A)

Hydrazine hydrate (1.5 g, 0.03 mol) was added to (20 ml) ethanolic solution of diacetyl mono oxime (3.03 g, 0.03mol) in three necks round flask (100 ml), then the mixture was refluxed with stirring for 6 hrs. The solid product was filtered off and recrystallization from Ethanol. The yield of the white product is 75%.

Synthesis of (2E,3Z)-3-(((1E,2E)-3-(2-((l1-oxidaneyl)-l5-methyl)phenyl)allylidene) hydrazineylidene)butan-2-one oxime ligand (L)

(15ml) ethanolic solution of 2-methoxycinnamaldehyde (0.01mol, 2.59g) with three drops of glacial acetic acid was mixing with (10ml) ethanolic solution of the compound (A) (0.01mol,1.62 g), then the reaction mixture was refluxed for three (hours). TLC was used to monitor the reaction. The resulting solid products was filtered off and recrystallization from ethanol, The yield of the yellow Schiff base product is 75%.

Synthesis of the transition meatal complexes

Adding a heated ethanolic ligand solution to an equimolar metal salt produced metal complexes. The mixture of reaction was heated and stirred for 3 hours. The products were vacuum-dried in anhydrous CaCl2 after filtering and washing with ethanol multiple times., and crystallize it using a heated ethanol solution

Result and Discussion

The ligand (L) was synthesized by a two steps synthetic strategy which has been outlined in Scheme (1), then the complexes was synthesized by condensation of

Indonesian Journal on Health Science and Medicine
Vol. 2 No. 1 (2025): January
ISSN 3063-8186. Published by Universitas Muhamamdiyah Sidoarjo

https://doi.org/10.21070/ijhsm.v2i1.60

the ligand with the acetate of different transition metals as shown in scheme (1).

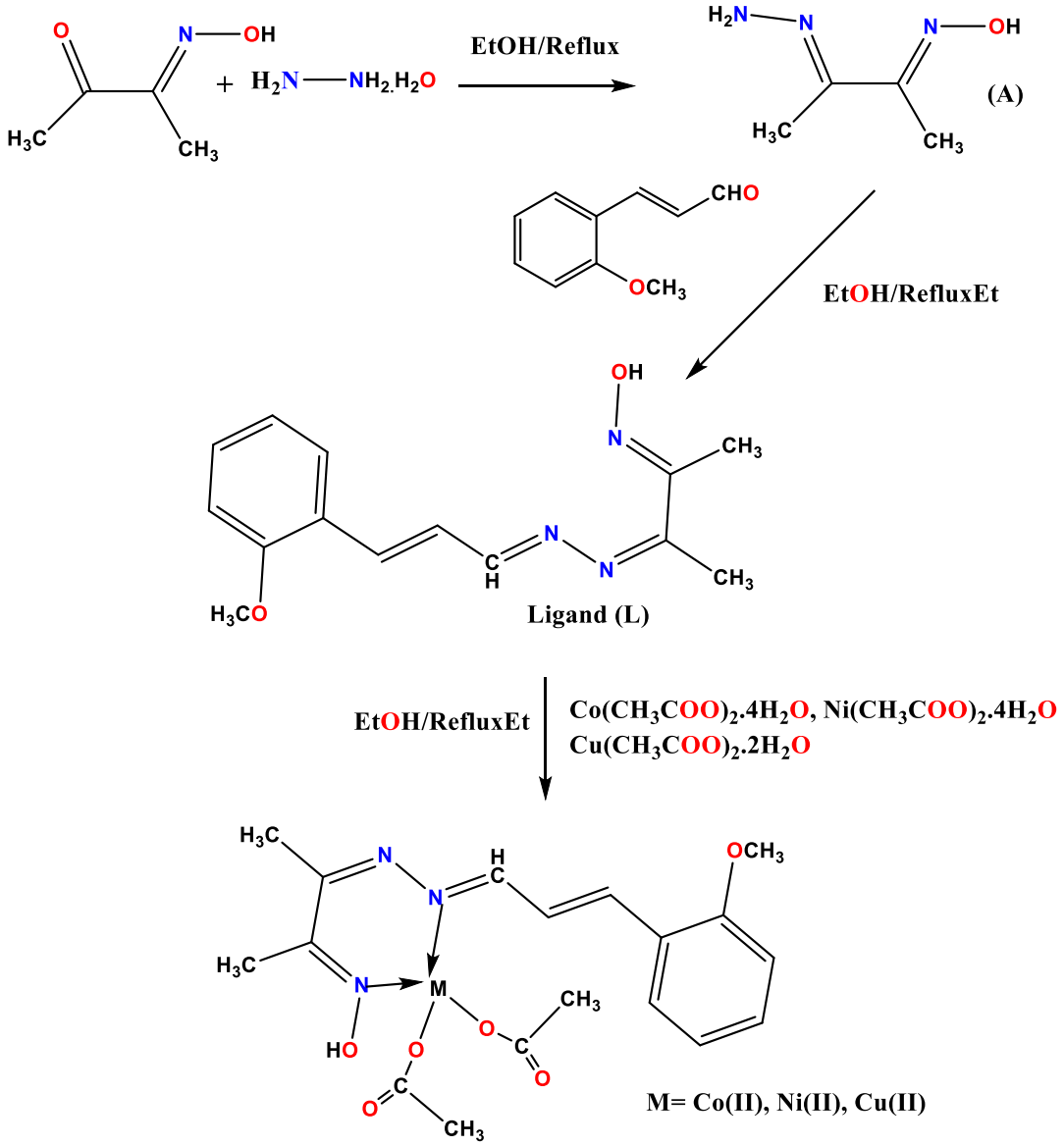

Scheme (1) Synthesis the ligand and its complexes

Table (1) shows elemental microanalysis (CHN), atomic absorption, conductivity, magnetic susptibility, and physical qualities. The complexes' molar conductance values in (10-3 M) DMSO range from 8 to 17 Ω-1cm2mol-1, indicating non-electrolysis. Magnetic moment of Cu d9 is 1.7 B.M. Copper complex geometry was square planar, while cobalt complex geometry was tetrahedral because Co d7 has a magnetic moment of 4.62 B.M. while Ni has diamagnetic properties and square planer geometry.

Indonesian Journal on Health Science and Medicine
Vol. 2 No. 1 (2025): January
ISSN 3063-8186. Published by Universitas Muhamamdiyah Sidoarjo

https://doi.org/10.21070/ijhsm.v2i1.60

Table (1). analytical and physical measurement

comp	color	m.p °C	μeff B.M	Λ Scm 2. mol-1	C% exp C%(cal)	H% exp H%(cal)	N% exp N%(cal)	M%	%Yield
$C_{18}H_{17}N_5O_4$ Ligand (L)	yellow	D> 165			59.37 (58.85)	4.13 (4.66)	20.79 (19.06)		82
Co(L)($CH_3COO)_2$	brown	D> 194	4.6	15				12.68	61
Ni(L)($CH_3COO)_2$	green yellowish	D> 213	dia	11				13.92	57
Cu(L)($CH_3COO)_2$	green	D>219	1.7	13				15.8	51

D= Decomposition

Infrared spectra:

The data of Infrared spectra are depicted in table (2). The spectrum of ligand shows peaks of stretching vibration at 3748, 3005, 1622 and 1585 cm-1, which are assignable to v (O-H) oxime, v (C-H) aromatic, v (C=N) imine and v (C=N) oxime respectively as shown in Fig. (1). The stretching vibration of the complexes demonstrated the shift of azomethine groups v (C = N) to the higher frequencies as shown in Table (2). The spectra of complexes demonstrated new band vibrational modes at (565-578) cm-1 and (450-480) cm-1 are assignable to the M-N and M-O group frequencies as a result of bonding the metal ion with the ligand.

Table (2). FTIR frequencies data for the ligand and its metal complexes in (cm-1)

Comp.	v(O-H) oxime	v(C-H) aromatic	v(C=N) imine	v(C=N) oxime	v(M-N)	v(M-O)
ligand	3740	3005	1622	1585		

Indonesian Journal on Health Science and Medicine
Vol. 2 No. 1 (2025): January
ISSN 3063-8186. Published by Universitas Muhamamdiyah Sidoarjo

https://doi.org/10.21070/ijhsm.v2i1.60

$Co(L)(CH_3COO)_2$	3738	3026	1627	1587	572	480
$Ni(L)(CH3COO)_2$	3745	3005	1631	1687	565	450
$Cu(L)(CH3COO)_2$	3748	3032	1625	1587	578	460

Fig.(1) FTIR spectrum of ligand

Proton Nuclear Magnetic Resonance of ligand (1H-NMR)

1H- NMR Spectrum of the ligand were recorded in DMSO-d6 solution as shown in fig. (2) The spectrum appeared a singlet signal at δ (8.37) ppm due to the proton of (OH) oxime group, doublet signal at δ (8.35) ppm due to the proton of azomethine group (N = CH), multisignals at δ (7.10-8.34) ppm belong to aromatic protons, doublet signals at the region δ (6.99.37-7.09) ppm are a suitable for olivanic proton of (HC=CH) group, the proton of methoxy (O-CH3) group seemed at δ (3.89) ppm, tow signals at δ (2.09) ppm and δ (3.18) ppm for methyl groups (CH3).

Indonesian Journal on Health Science and Medicine
Vol. 2 No. 1 (2025): January
ISSN 3063-8186. Published by Universitas Muhamamdiyah Sidoarjo

https://doi.org/10.21070/ijhsm.v2i1.60

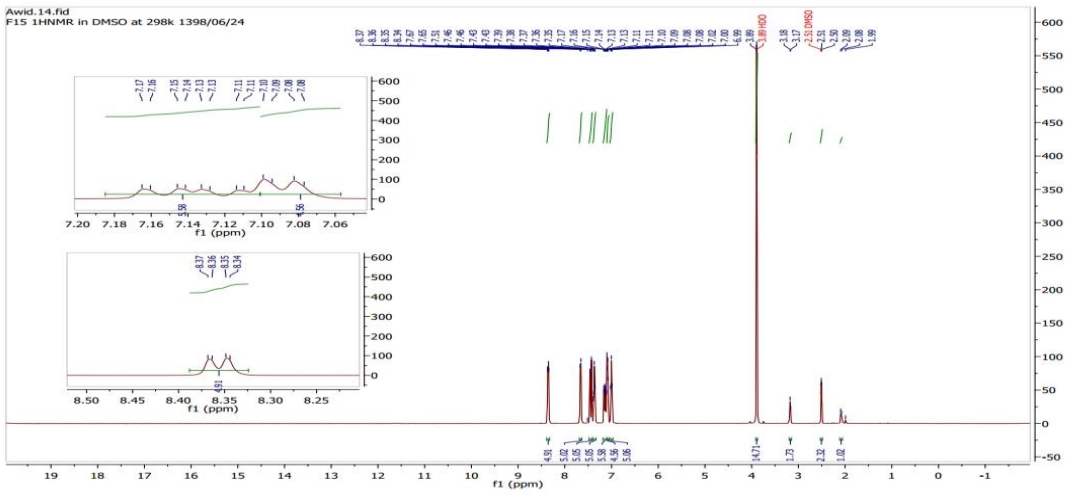

Fig. (2) 1H-NMR spectrum of the ligand

Mass spectra

The mass spectrum exhibited molecular ion of the ligand at 259 m/z corresponding to its chemical formula [C14H17N3O2] +, the spectrum showed a high intensity peak at 41 m/z in a good agreement with chemical formula [C2H3N]+. Other peaks are due to the subsequent fragmentation as shown in scheme (2) and Fig. (3).

The structure of complexes is confirmed by the help of mass spectra, the mass spectrum of Co (II) complex. exhibited a peak at 436 m/z which is due molecular ion of the formula Co(C14H17N3O2)(CH3COO)2.

The mass spectrum of the Ni (II) complex exhibited a peak at 437 m/z which is due molecular ion of the formula Ni(C14H17N3O2)(CH3COO)2.

The mass spectrum of the Cu (II) complex exhibited a peak at 444 m/z which is due molecular ion of the formula Cu(C14H17N3O2)(CH3COO)2.

Indonesian Journal on Health Science and Medicine
Vol. 2 No. 1 (2025): January
ISSN 3063-8186. Published by Universitas Muhamamdiyah Sidoarjo

https://doi.org/10.21070/ijhsm.v2i1.60

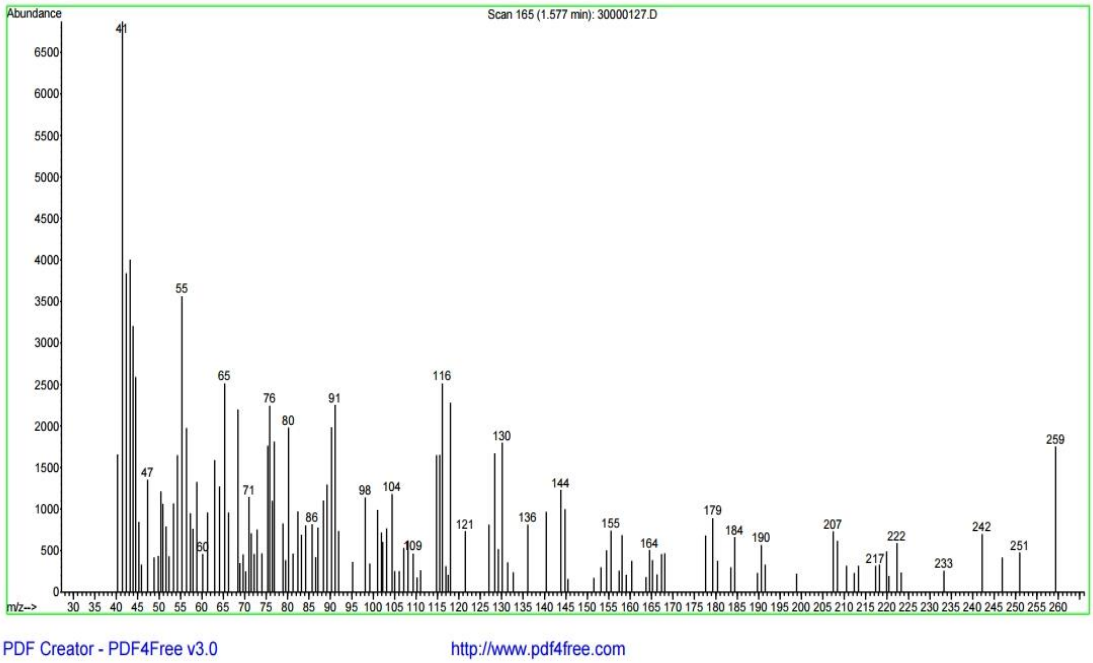

Fig. (3) mass spectrum of the ligand

Indonesian Journal on Health Science and Medicine
Vol. 2 No. 1 (2025): January
ISSN 3063-8186. Published by Universitas Muhamamdiyah Sidoarjo

https://doi.org/10.21070/ijhsm.v2i1.60

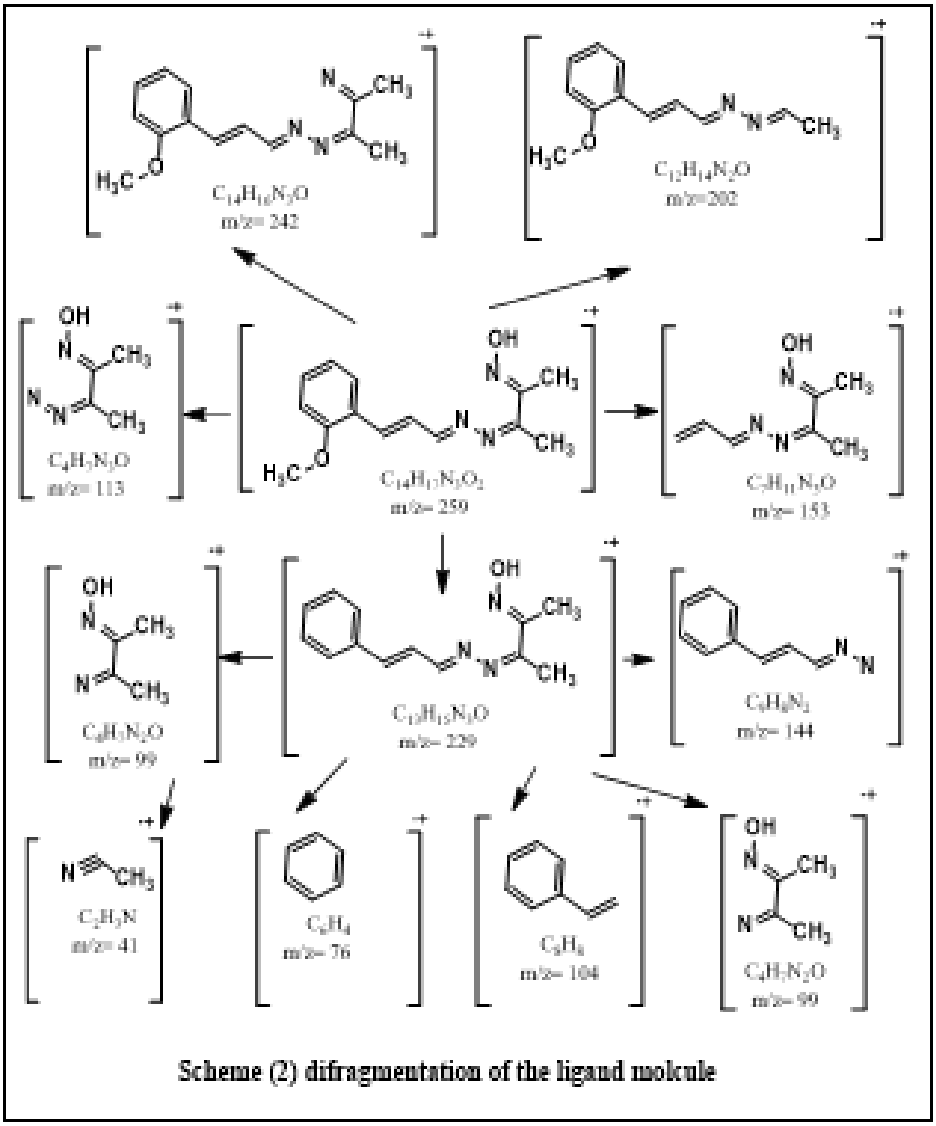

Scheme (2) difragmentation of the ligand molcule

Cytotoxic studies-MTT assay

Cytotoxicity experiments on new ligand (oxime) against breast cancer (MCF-7) and normal cells (WRL68) are given in table (3) and fig. (4). MTT (3-[4,5-dimethylthiazolyl]-2,5-diphenyltetrazolium bromide) reduction was measured by using the modified cell viability (MTT) method indicated by (Kumar et al, 2018)[19]. The density of 1*105 cells/well was seeded on 96-well transparent flat-bottom plates (Greiner Bio-One, Frickenhausen, Germany) for 24 hours. After 24 hours at 37°C, the cells were treated with various concentration of the ligand (100, 200, 300, 400, and 500 µg/ml) following medium extraction. The medium was removed from the plate after 48 hours at 37°C. In a serum-free medium, to each well was added 200 µl of MTT reagent (1

Indonesian Journal on Health Science and Medicine
Vol. 2 No. 1 (2025): January
ISSN 3063-8186. Published by Universitas Muhamamdiyah Sidoarjo

https://doi.org/10.21070/ijhsm.v2i1.60

mg/ml). After 4 hours the medium was removed and 200 µl of (DMSO) was added to each well. The metabolized MTT agent dissolved in DMSO was measured at 570 nm by a microplate reader. Each concentration was tested three times. The optical density (OD) of each well was measured using an ELISA plate reader (infinite F50, TECAN, Austria). (mean OD of treated cells/mean OD of untreated cells) x100 = % cell viability[20]. The 50% inhibitory concentration (IC50) values were determined and plotted using a sigmoidal dose-response equation. Assaying cell viability. The ligand decreased tumor cell viability at 500 µg/ml, achieving 51.2% cytotoxic effectiveness. In contrast, normal cellular cells had (74.8) at the same dose, while (100 µg/ml) inhibited the least. Comparing the IC50 values for each cell line yielded, which reflects the compound's cytotoxicity against cancer cells but safety against normal cells. The ligand selectively cytotoxic against cancer cell lines (IC50 = 103 µg/ml) and less active against normal cells (IC50 = 217 µg/ml).

Tables (3) give percent of the viability rate values for the ligand after 24 hours of treatment with various centration

Concentration	(MCF-7)		(WRL68)	
	mean	SD	mean	SD
500	51.2	0.98	74.8	3.70
400	65.4	1.20	81.7	3.12
300	79.21	0.35	86.2	3.009
200	86.8	0.82	93.8	0.77
100	92.9	0.41	96.2	0.71

Indonesian Journal on Health Science and Medicine
Vol. 2 No. 1 (2025): January
ISSN 3063-8186. Published by Universitas Muhamamdiyah Sidoarjo

https://doi.org/10.21070/ijhsm.v2i1.60

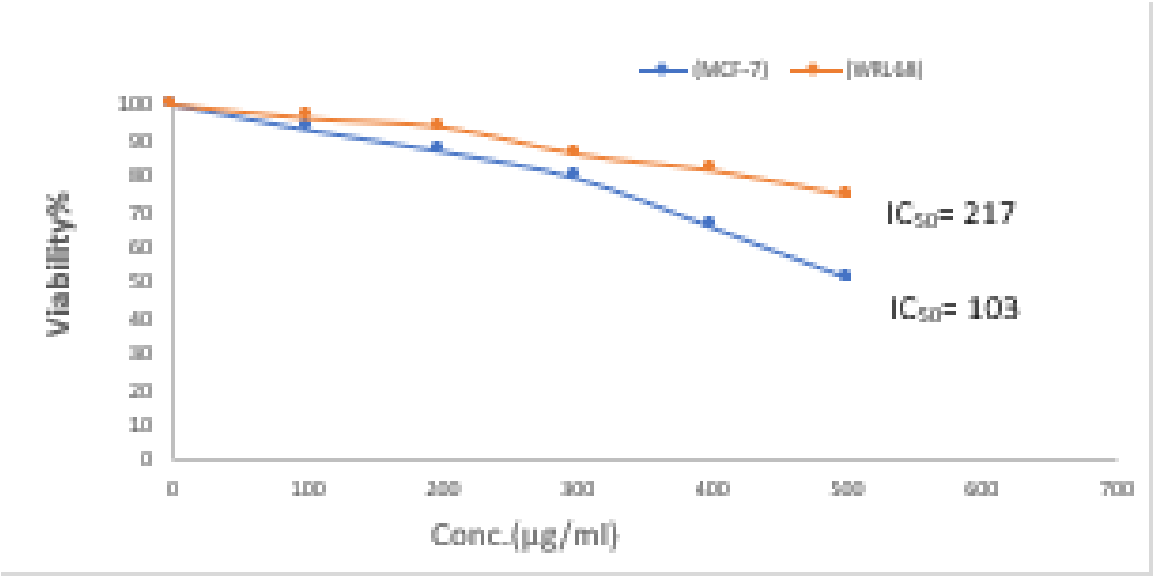

Fig.(4) Cytotoxicity of the ligand against breast cancer (MCF-7) and normal cells (WRL68)

Molecular modeling

Density functional theory (DFT) calculations for ligand and its metal complexes were carried out at B3LYP/6-31G+(d,p) method using Gaussian 09 quantum mechanical, The bond lengths, bond angles and geometrical structures are shown in fig.(5) and table (4). The ofcalculations Natural charge revealed the presence of differently charged regions in the ligand, as indicated by 2D electrostatic surface shown in Fig. (5). The theoretically calculated frontier molecular orbitals (HOMO and LUMO) in the ground state are illustrated Fig.(5-8). Based on HOMO and LUMO energies, the energy gab (ΔE = ELUMO - EHOMO), ionization potential (I = -EHOMO), electron affinity (A = -ELUMO), Electro negativity (χ= (I+A)/2), chemical potential (μ = -χ = -(I + A)/2), global hardness (η = (I - A)/2), global softness (1/2η) as well as electrophilicity index (ω = μ2/2η) reactivity indices were calculated at the same level and shown in table (7). The smaller value of the energy gap explains the charge transfer interactions that take place inside the molecule and affect its biological activity. The energy gap reflects the chemical activity of the molecule. A molecule is considered soft if it has a small border orbital gap and is generally associated with high chemical reactivity.[21].

Indonesian Journal on Health Science and Medicine
Vol. 2 No. 1 (2025): January
ISSN 3063-8186. Published by Universitas Muhamamdiyah Sidoarjo

https://doi.org/10.21070/ijhsm.v2i1.60

Table (4) Bond lengths (Å) and angles (◦) for the ligand (L)

Bond length	Vvalue	Bond length	Value	Bond angles	Value	Bond angles	Value
C1-C2	1.397	C20-N21	1.286	C1-C2-C3	119.427	C20-C19-N18	116.743
C2-C3	1.392	N21-O22	1.411	C2-C3-C4	121.997	N21-C20-C19	115.726
C3-C4	1.407	O22-H23	0.097	C3-C4-C5	117.527	O22-N21-C20	112.579
C4-C5	1.422	C19-C24	1.511	C1-C2-C6	120.358	H23-O22-N21	102.059
C1-C6	1.397	C24-H25	1.511	H7-C1-C2	120.341	C24-C19-N18	125.915
C1-H7	1.087	N18-C19	1.294	H8-C2-C1	120.467	H25-C24-C19	110.422
C2-H8	1.085	C19-C20	1.494	H9-C3-C2	119.103	C26-C20-C19	118.652
C3-H9	1.085	C20-C26	1.508	H10-C6-C1	119.391	H27-C28-C20	110.034
C6-H10	1.083	C26-H27	1.096	C11-C4-C3	122.980	H28-C24-C19	110.704
C4-C11	1.461	C24-H28	1.095	C12-C11-C4	127.055	H29-C26-C20	111.057
C11-C12	1.356	C26-H29	1.088	H13-C11-C4	115.254	H30-C24-C19	110.256
C11-H13	1.086	C24-H30	1.088	H14-C12-C11	122.257	H31-C26-C20	59.974
C12-H14	1.087	C26-H31	1.095	C15-C12-C11	121.730	O32-C5-C4	116.075
C12-C15	1.441	C5-O32	1.366	H16-C15-C12	119.124	C33-O32-C5	119.163
C15-H16	1.095	C33-O32	1.423	N17-C15-C12	121.033	H34-C33-O32	105.655
C15-N17	1.296	C33-H34	1.090	N18-N17-C15	111.495	H35-C33-O32	111.354
N16-N18	1.391	C33-H35	1.097	C19-N18-C15	114.820	H36-C33-O32	111.267
Dihedral		Value	Dihedral		Value	Dihedral	Value
C1-C2-C3-C4		0.089	C11-C12-C15-H16		-0.154	N18-C19-C24-H28	136.828
C2-C3-C4-C5		-0.124	C11-C12-C15-N17		179.689	C19-C20-C26-H29	-179.11
C1-C2-C3-C6		0.036	C12-C15-N17-N18		179.982	N18-C19-C24-H30	14.856

Indonesian Journal on Health Science and Medicine
Vol. 2 No. 1 (2025): January
ISSN 3063-8186. Published by Universitas Muhamamdiyah Sidoarjo

https://doi.org/10.21070/ijhsm.v2i1.60

C1-C2-C3-H7	179.977	C15-N17-N18-C19	177.193	C19-C20-C26-H31	59.954
C1-C2-C6-H8	-179.835	N17-N18-C19-C20	178.993	C3-C4-C5-O32	179.929
C1-C2-C3-H9	-179.665	N18-C19-C20-N21	-44.950	C4-C5-O32-C33	-179.99
C1-C2-C6-H10	-179.989	C19-C20-N21-O22	179.205	C5-O32-C33-H34	179.712
C2-C3-C4-C11	179.932	C20-N21-O22-H23	178.613	C5-O32-C33-H35	-61.472
C3-C4-C311-C12	-3.449	N17-N18-C19-C24	-2.414	C5-O32-C33-H36	61.167
C3-C4-C11-H13	176.719	N18-C19-C24-H25	-104.59		
C4-C11-C12-H14	-0.443	N18-C19-C20-C26	136.247		
C4-C11-C12-C15	179.820	C19-C20-C26-H27	-58.306		

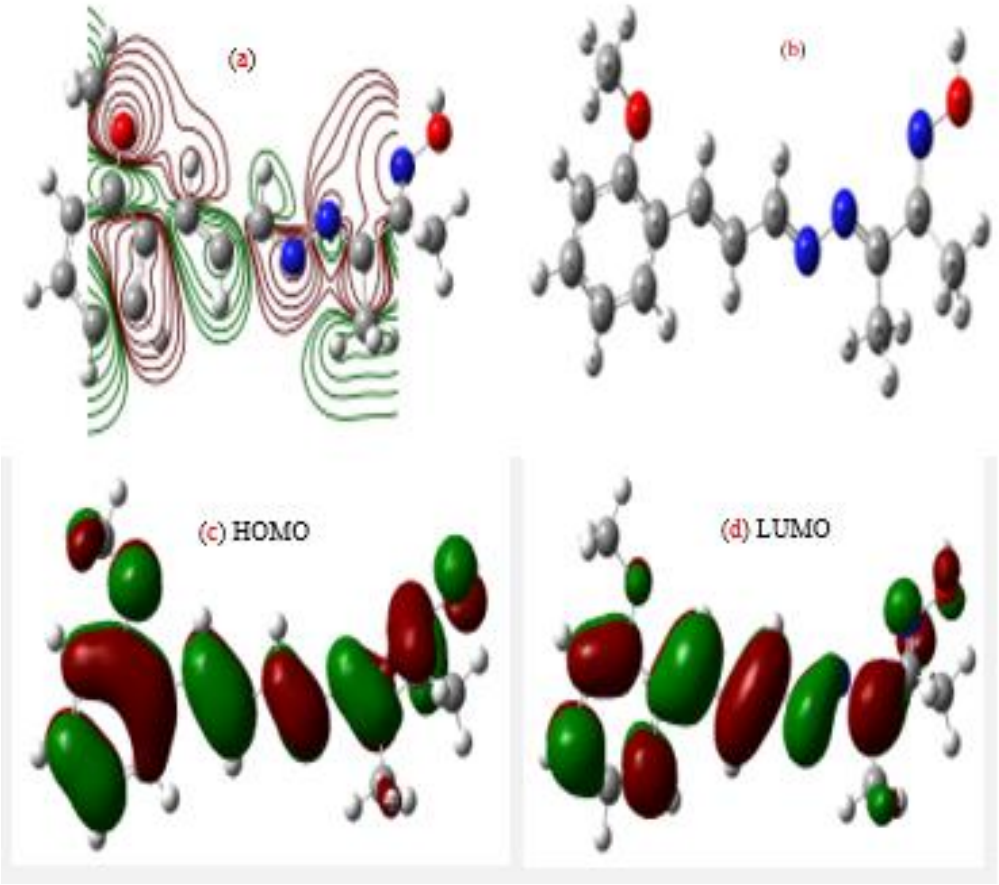

Fig. (5) (a) the geometry optimization structure, (b) 2D electrostatic surface, (c) HOMO and (d) LUMO orbital of the ligand

Indonesian Journal on Health Science and Medicine
Vol. 2 No. 1 (2025): January
ISSN 3063-8186. Published by Universitas Muhamamdiyah Sidoarjo

https://doi.org/10.21070/ijhsm.v2i1.60

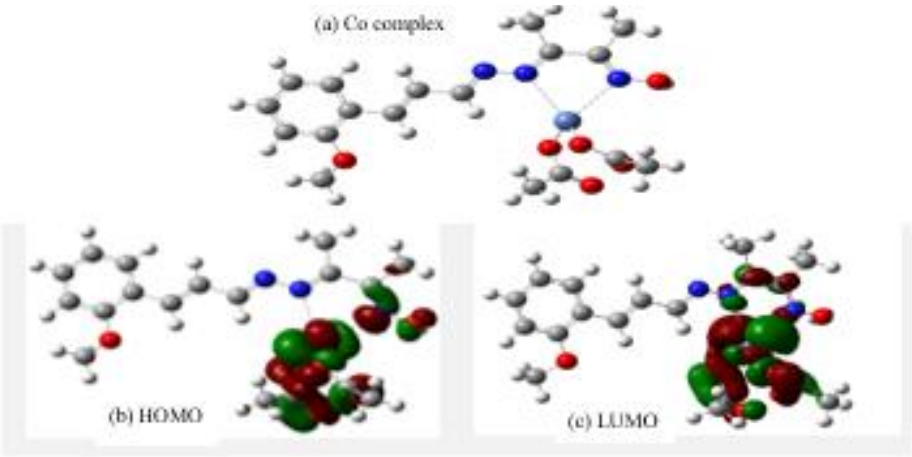

Fig. (6) (a) the geometry optimization structure, (b) HOMO and (c) LUMO orbital of the Co(II) complex

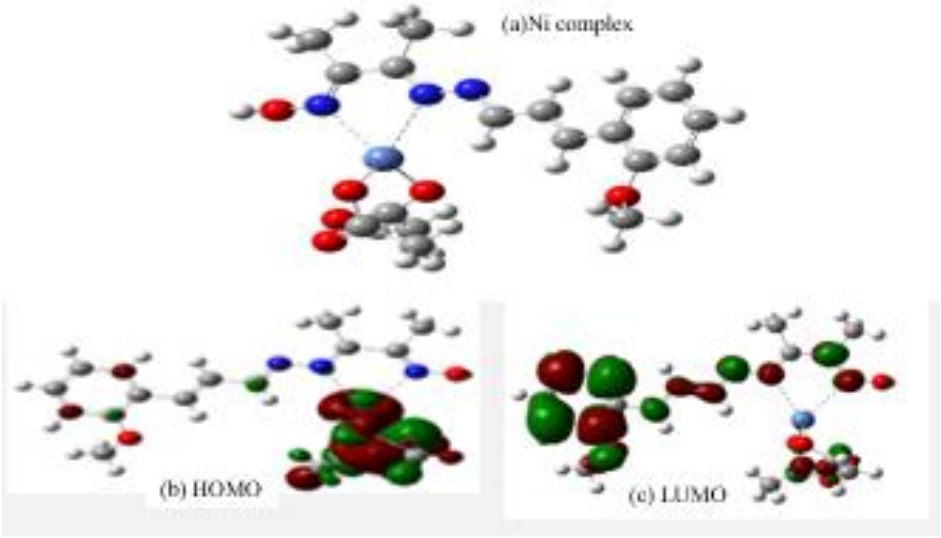

Fig. (7) (a) the geometry optimization structure, (b) HOMO and (c) LUMO orbital of the Ni(II) complex

Indonesian Journal on Health Science and Medicine
Vol. 2 No. 1 (2025): January
ISSN 3063-8186. Published by Universitas Muhamamdiyah Sidoarjo

https://doi.org/10.21070/ijhsm.v2i1.60

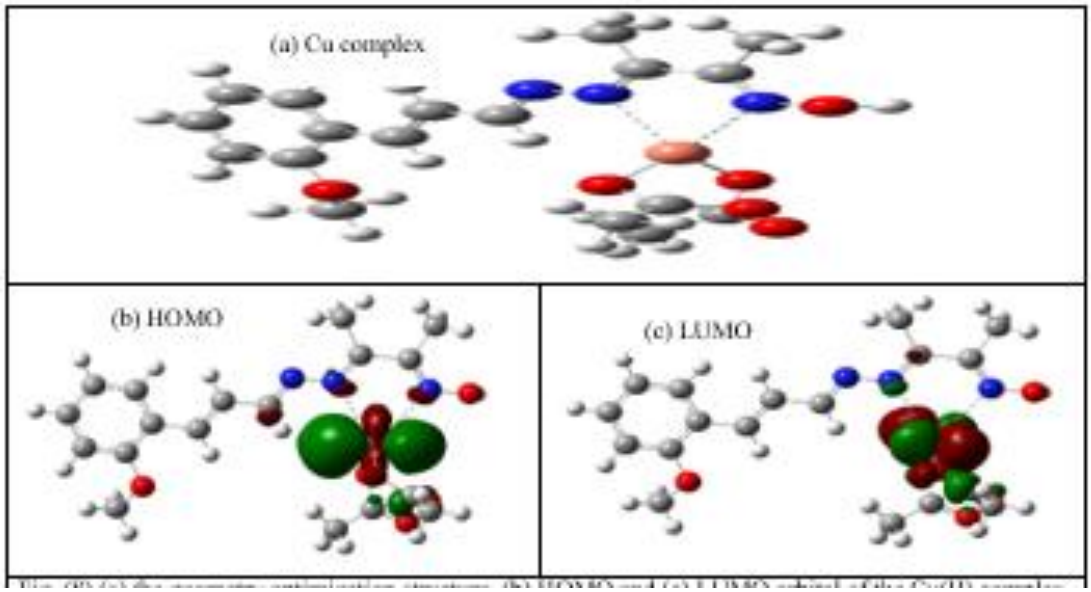

Fig. (8) (a) the geometry optimization structure, (b) HOMO and (c) LUMO orbital of the Cu(II) complex

Table (5) global parameters of the ligand and its metal complexes using B3LYP/6-31G calculated

Parameter	Value	Co complex	Ni complex	Cu complex
E_{HOMO} (eV)	-5.8121	-7.5137	-5.2205	-5.5571
E_{HOMO} -1 (eV)	-6.2688	-7.6299	-5.2722	-5.5842
E_{LUMO} (eV)	-2.2213	-5.3291	-3.0687	-3.3679
E_{LUMO} +1 (eV)	0.2304	-4.6051	-3.0241	-3.2642
ΔE (LLUMO - HOMO) (eV)	3.5908	2.1846	2.1518	2.2929
ΔE (LLUMO - HOMO) (eV)	5.4435	3.0248	2.2481	2.3200
Ionisation potential, I (eV)	+5.8121	+7.51369	5.2205	5.5571
Electron affinity, A (eV)	+2.2213	+5.3291	3.0687	3.3679
Electro negativity, χ (eV)	4.0162	6.4214	4.1446	4.4625
Chemical potential, μ (eV)	-4.0162	_6.4214	-4.1446	-4.4625
Global hardness, η (eV)	1.7954	1.0923	1.0759	1.0946

ISSN 3063-8186. Published by Universitas Muhamamdiyah Sidoarjo

https://doi.org/10.21070/ijhsm.v2i1.60

Global softness, S (eV)	0.2785	0.4577	0.4647	0.4568
electrophilicity index, ω (eV)	4.4919	18.875	7.9829	9.0964

Conclusion

A new Schiff base had been prepared. The spectroscopic study has characterized the structure of the Schiff base ligand (L1) coordinates with metal ions through azomethine nitrogen atom. elemental analyses (C, H, N), molar conductance measurements, IR, and 1H NMR spectroscopic). All the complexes have an electrolytic nature. The complexes exhibit tetrahedral geometry for Co and square planer for Ni and Cu

References

[1] N. P. P. and S. A. S. Kalaivani, "SCHIFF BASES: FACILE SYNTHESIS, SPECTRAL CHARACTERIZATION AND BIOCIDAL STUDIES," IJAGPT, vol. 3, no. 1, pp. 219–223, 2012.

[2] S. Slassi, A. Fix-Tailler, G. Larcher, A. Amine, and A. El-Ghayoury, "Imidazole and Azo-Based Schiff Bases Ligands as Highly Active Antifungal and Antioxidant Components," Heteroatom Chemistry, vol. 2019, pp. 1–8, Jan. 2019, doi: 10.1155/2019/6862170.

[3] G. , S. R. R. R. and K. R. Valarmathy, "Synthesis of Schiff base (E)-2-(((3-Hydroxyphenyl)imino)methyl)-6-methoxyphenol Containing N and O Donors and its Metal Complexes: Spectral, Thermal, Redox Behaviour, Fluorescence Quenching, Antimicrobial and Anticancer Studies Fluorescence Quenching, Antimicrobial and Anticancer Studies," Asian .J. chem, vol. 30, pp. 645–650, 2018.

[4] L. S. Ashoor, R. A. Majeed, and R. K. R. Al-Shemary, ""Applications of biological of Azo-Schiff base ligand and its metal complexes and: A review "," Muthanna J Pure Sci, vol. 8, no. 1, pp. 74–80, Jan. 2021, doi: 10.52113/2/08.01.2021/74-90.

[5] F. K. Ommenya, E. A. Nyawade, D. M. Andala, and J. Kinyua, "Synthesis, Characterization and Antibacterial Activity of Schiff Base, 4-Chloro-2-{(E)-[(4-Fluorophenyl)imino]methyl}phenol Metal (II) Complexes," J Chem, vol. 2020, pp. 1–8, Mar. 2020, doi: 10.1155/2020/1745236.

ISSN 3063-8186. Published by Universitas Muhamamdiyah Sidoarjo

https://doi.org/10.21070/ijhsm.v2i1.60

[6] L. Wei et al., "Antifungal activity of double Schiff bases of chitosan derivatives bearing active halogeno-benzenes," Int J Biol Macromol, vol. 179, pp. 292–298, May 2021, doi: 10.1016/j.ijbiomac.2021.02.184.

[7] S. J. Hamid and T. Salih, "Design, Synthesis, and Anti-Inflammatory Activity of Some Coumarin Schiff Base Derivatives: In silico and in vitro Study," Drug Des Devel Ther, vol. Volume 16, pp. 2275–2288, Jul. 2022, doi: 10.2147/DDDT.S364746.

[8] S. Murtaza, M. S. Akhtar, F. Kanwal, A. Abbas, S. Ashiq, and S. Shamim, "Synthesis and biological evaluation of schiff bases of 4-aminophenazone as an anti-inflammatory, analgesic and antipyretic agent," Journal of Saudi Chemical Society, vol. 21, pp. S359–S372, Jan. 2017, doi: 10.1016/j.jscs.2014.04.003.

[9] M. S. Tople, N. B. Patel, P. P. Patel, A. C. Purohit, I. Ahmad, and H. Patel, "An in silico-in vitro antimalarial and antimicrobial investigation of newer 7-chloroquinoline based Schiff-bases," J Mol Struct, vol. 1271, p. 134016, Jan. 2023, doi: 10.1016/j.molstruc.2022.134016.

[10] S. Kaushik, S. K. Paliwal, M. R. Iyer, and V. M. Patil, "Promising Schiff bases in antiviral drug design and discovery," Medicinal Chemistry Research, vol. 32, no. 6, pp. 1063–1076, Jun. 2023, doi: 10.1007/s00044-023-03068-0.

[11] I. A. Seliem et al., "Development of Isatin-Based Schiff Bases Targeting VEGFR-2 Inhibition: Synthesis, Characterization, Antiproliferative Properties, and QSAR Studies," ChemMedChem, vol. 17, no. 13, Jul. 2022, doi: 10.1002/cmdc.202200164.

[12] D. Iacopetta et al., "Schiff Bases: Interesting Scaffolds with Promising Antitumoral Properties," Applied Sciences, vol. 11, no. 4, p. 1877, Feb. 2021, doi: 10.3390/app11041877.

[13] A. M. Hassan, A. O. Said, B. H. Heakal, A. Younis, W. M. Aboulthana, and M. F. Mady, "Green Synthesis, Characterization, Antimicrobial and Anticancer Screening of New Metal Complexes Incorporating Schiff Base," ACS Omega, vol. 7, no. 36, pp. 32418–32431, Sep. 2022, doi: 10.1021/acsomega.2c03911.

[14] M. H. Raheema, N. A. Khudhair, T. H. AL-Noor, S. R. Al-Ayash, H. H. Kharnoob, and S. M. H. Obed, "Enhancement of corrosion protection of metal carbon steel C45 and stainless steel 316 by using inhibitor (Schiff base) in sea water," Baghdad

ISSN 3063-8186. Published by Universitas Muhamamdiyah Sidoarjo

https://doi.org/10.21070/ijhsm.v2i1.60

Science Journal, vol. 20, no. 3(Suppl.), p. 1012, Jun. 2023, doi: 10.21123/bsj.2023.7749.

[15] K. M. Abuamer, A. A. Maihub, M. M. El-Ajaily, A. M. Etorki, M. M. Abou-Krisha, and M. A. Almagani, "The Role of Aromatic Schiff Bases in the Dyes Techniques," Int J Org Chem (Irvine), vol. 04, no. 01, pp. 7–15, 2014, doi: 10.4236/ijoc.2014.41002.

[16] J. Anacona and J. Santaella, "Synthesis, magnetic and spectroscopic studies of a Schiff base derived from cephaclor and 1,2-diaminobenzene and its transition metal complexes," Spectrochim Acta A Mol Biomol Spectrosc, vol. 115, pp. 800–804, Nov. 2013, doi: 10.1016/j.saa.2013.06.107.

[17] G. Sundararajan, D. Rajaraman, T. Srinivasan, D. Velmurugan, and K. Krishnasamy, "Synthesis, characterization, computational calculation and biological studies of some 2,6-diaryl-1-(prop-2-yn-1-yl)piperidin-4-one oxime derivatives," Spectrochim Acta A Mol Biomol Spectrosc, vol. 139, pp. 108–118, Mar. 2015, doi: 10.1016/j.saa.2014.12.014.

[18] L. Di Costanzo, M. Moulin, M. Haertlein, F. Meilleur, and D. W. Christianson, "Expression, purification, assay, and crystal structure of perdeuterated human arginase I," Arch Biochem Biophys, vol. 465, no. 1, pp. 82–89, Sep. 2007, doi: 10.1016/j.abb.2007.04.036.

[19] P. Kumar, A. Nagarajan, and P. D. Uchil, "Analysis of Cell Viability by the MTT Assay," Cold Spring Harb Protoc, vol. 2018, no. 6, p. pdb.prot095505, Jun. 2018, doi: 10.1101/pdb.prot095505.

[20] L. Gasparini et al., "In vitro cell viability by CellProfiler ® software as equivalent to MTT assay," Pharmacogn Mag, vol. 13, no. 50, p. 365, 2017, doi: 10.4103/0973-1296.210176.

[21] E. M. Abdalla, S. S. Hassan, H. H. Elganzory, S. A. Aly, and H. Alshater, "Molecular Docking, DFT Calculations, Effect of High Energetic Ionizing Radiation, and Biological Evaluation of Some Novel Metal (II) Heteroleptic Complexes Bearing the Thiosemicarbazone Ligand," Molecules, vol. 26, no. 19, p. 5851, Sep. 2021, doi: 10.3390/molecules26195851.